Chemistry Europe
European Chemical Societies Publishing

WILEY VCH

Excellence in Chemistry Research

Announcing our new flagship journal

- Gold Open Access
- Publishing charges waived
- Preprints welcome
- Edited by active scientists

Meet the Editors of *ChemistryEurope*

Luisa De Cola
Università degli Studi di Milano Statale, Italy

Ive Hermans
University of Wisconsin-Madison, USA

Ken Tanaka
Tokyo Institute of Technology, Japan

Chemistry–A European Journal
Research Article
doi.org/10.1002/chem.202203734
Chemistry Europe
European Chemical Societies Publishing
www.chemeurj.org

Two Rings Around One Ball: Stability and Charge Localization of [1:1] and [2:1] Complex Ions of [10]CPP and $C_{60/70}$[*]

Markus Freiberger[+],[a] Martin B. Minameyer[+],[a] Iris Solymosi,[b] Stefan Frühwald,[c] Marcel Krug,[a] Youzhi Xu,[d] Andreas Hirsch,[b] Timothy Clark,[e] Dirk M. Guldi,[a] Max von Delius,[d] Konstantin Amsharov,[f] Andreas Görling,[c] M. Eugenia Pérez-Ojeda,*[b] and Thomas Drewello*[a]

In memory of the late Dr. Roman I. Flyunt, a dear colleague and friend.

Abstract: We investigate the gas-phase chemistry of non-covalent complexes of [10]cycloparaphenylene ([10]CPP) with C_{60} and C_{70} by means of atmospheric pressure photoionization and electrospray ionization mass spectrometry. The literature-known [1:1] complexes, namely [10]CPP⊃C_{60} and [10]CPP⊃C_{70}, are observed as radical cations and anions. Their stability and charge distribution are studied using energy-resolved collision-induced dissociation (ER-CID). These measurements reveal that complexes with a C_{70} core exhibit a greater stability and, on the other hand, that the radical cations are more stable than the respective radical anions. Regarding the charge distribution, in anionic complexes charges are exclusively located on C_{60} or C_{70}, while the charges reside on [10]CPP in the case of cationic complexes. [2:1] complexes of the $([10]CPP_2⊃C_{60/70})^{+\bullet/-\bullet}$ type are observed for the first time as isolated solitary gas-phase species. Here, C_{60}-based [2:1] complexes are less stable than the respective C_{70} analogues. By virtue of the high stability of cationic [1:1] complexes, [2:1] complexes show a strongly reduced stability of the radical cations. DFT analyses of the minimum geometries as well as molecular dynamics calculations support the experimental data. Furthermore, our novel gas-phase [2:1] complexes are also found in 1,2-dichlorobenzene. Insights into the thermodynamic parameters of the binding process as well as the species distribution are derived from isothermal titration calorimetry (ITC) measurements.

Introduction

Recent synthetic progress has paved the way towards an amazing array of strained, carbon-based nano-structures with bent π systems, for example, solitary and fused rings, catenanes and even knots.[1–5] Among them, ring molecules are of special interest. Showing intriguing photophysical and electronic properties, they are, for example, promising for new optoelectronic applications.[6–12] Moreover, ring molecules, also referred to as nanohoops, have advanced as new protagonists in the

[a] M. Freiberger,[+] M. B. Minameyer,[+] M. Krug, Prof. Dr. D. M. Guldi, Prof. Dr. T. Drewello
Physical Chemistry I
Department of Chemistry and Pharmacy
Friedrich-Alexander-Universität Erlangen-Nürnberg
Egerlandstraße 3, 91058 Erlangen (Germany)
E-mail: thomas.drewello@fau.de

[b] I. Solymosi, Prof. Dr. A. Hirsch, Dr. M. E. Pérez-Ojeda
Organic Chemistry II
Department of Chemistry and Pharmacy
Friedrich-Alexander-Universität Erlangen-Nürnberg
Nikolaus-Fiebiger-Straße 10, 91058 Erlangen (Germany)
E-mail: eugenia.perez-ojeda@fau.de

[c] Dr. S. Frühwald, Prof. Dr. A. Görling
Theoretical Chemistry
Department of Chemistry and Pharmacy
Friedrich-Alexander-Universität Erlangen-Nürnberg
Egerlandstraße 3, 91058 Erlangen (Germany)

[d] Dr. Y. Xu, Prof. Dr. M. von Delius
Institute of Organic Chemistry
Ulm University
Albert-Einstein-Allee 11, 89081 Ulm (Germany)

[e] Prof. Dr. T. Clark
Computer-Chemistry-Center
Department of Chemistry and Pharmacy
Friedrich-Alexander-Universität Erlangen-Nürnberg
Nägelsbachstraße 25, 91052 Erlangen (Germany)

[f] Prof. Dr. K. Amsharov
Organic Chemistry
Institute of Chemistry
Martin-Luther-Universität Halle-Wittenberg
Kurt-Mothes-Strasse 2, 06120 Halle (Germany)

[+] Both authors contributed equally to the paper

Supporting information for this article is available on the WWW under https://doi.org/10.1002/chem.202203734

field of host-guest chemistry.[13] Aromatic cycloparaphenylenes (CPPs) are prominent representatives of this new class of nanohoops.[7,14–15] However, even nanohoops consisting of antiaromatic units have been recently reported.[16–18] To tune their molecular properties, CPPs have been chemically modified. In this context, the substitution of hydrogen by halides[19–26] as well as carbon by nitrogen[27–32] have been achieved. Additionally, introduction of electron-donating or withdrawing groups[33] and larger π-frameworks[34] into the ring molecule have been reported.

As hosts for numerous guest molecules such as smaller rings,[35–38] fullerenes,[38–43] fullerene dumbbells,[24,44–47] endohedral metallo fullerenes,[36,48–52] larger PAHs[53–55] and organic cations,[56] CPPs represent a tremendously important contribution to the world of noncovalent inclusion complexes. Bonding results from concave/convex π–π, CH–π and/or charge–π interactions between host and guest. The bond energy in some of these complexes can be quite substantial. For instance, the bond strength in [10]CPP⊃C_{60}, one of the most prominent CPP fullerene complexes, is determined to be approximately 50 kJ mol^{-1}.[39]

By introduction of matrix-assisted laser desorption/ionization (MALDI) and electrospray ionization (ESI) as soft ionization methods for the non-destructive analysis of CPPs, we have recently extended the experimental repertoire for the study of CPPs and their noncovalent complexes by mass spectrometry-based gas-phase studies. For instance, MS^2 experiments provided evidence for a [10]CPP that is firmly interlocked within a [2]rotaxane.[46] Furthermore, we were able to determine the relative bond strength of a CPP-based porphyrinoid host molecule to C_{60}[57] as well as the relative bond strength between the host molecules [10]CPP, aza[10]CPP and methyl-aza[10]CPP and the C_{60} guest.[32]

In this study, CPP⊃fullerene complexes are investigated by atmospheric pressure photoionization (APPI) and electrospray ionization (ESI) mass spectrometry (MS) in combination with density functional theory (DFT). We are able to observe stable [2:1] complexes in which two CPPs encapsulate one fullerene. The charge distribution in [1:1] and [2:1] complexes between [10]CPP and fullerenes is elucidated for cations and anions and the relative stabilities of the complexes are established by energy-resolved collision-induced dissociation (ER-CID) experiments. In addition, the formation of the [2:1] complexes is studied in solution using isothermal titration calorimetry (ITC) and the thermodynamic parameters of the binding process are determined.

Results and Discussion

Figures 1a and b display the positive-ion mode mass spectra of solutions containing [10]CPP and C_{60} as well as [10]CPP and C_{70}, respectively. The most prominent signal in both spectra (at *m/z* 760.3) is assigned to $CPP^{+\bullet}$. CPP ionization is preferred due to the much lower ionization energy (IE) of the CPP compared to the fullerenes.[38] The signals at *m/z* 1481.3 and 1601.3 corroborate the existence of [1:1] complexes, $([10]CPP⊃C_{60/70})^{+\bullet}$. Interestingly, we also find signals at *m/z* 2242.6 and 2362.6 due to the formation of the [2:1] complexes, $([10]CPP_2⊃C_{60/70})^{+\bullet}$. Our observations provide clear evidence for their existence in the gas-phase, which has already been suggested in earlier solution-based experiments.[46] MS^1 spectra were also recorded in negative-ion mode (see Figure S1 in Supporting Information), in which signals corresponding to [1:1] as well as to [2:1] complexes are also present.

For noncovalent host-guest complexes, the cleavage of the noncovalent bonding between the host and the guest molecule represents the energetically most feasible dissociation reaction and leads to the separation of two separate entities. Since mass spectrometry is based on the detection of ions, it is a powerful tool to reveal the charge distribution in the dissociating complex. Figure 2 shows the result of collision-induced dissociation (CID) of the C_{60}-based [1:1] complex in the positive- (Figure 2a) and negative-ion mode (Figure 2b). In the positive-ion mode, the positive charge is generated by releasing an electron in the ionization event. The resulting ion is the radical

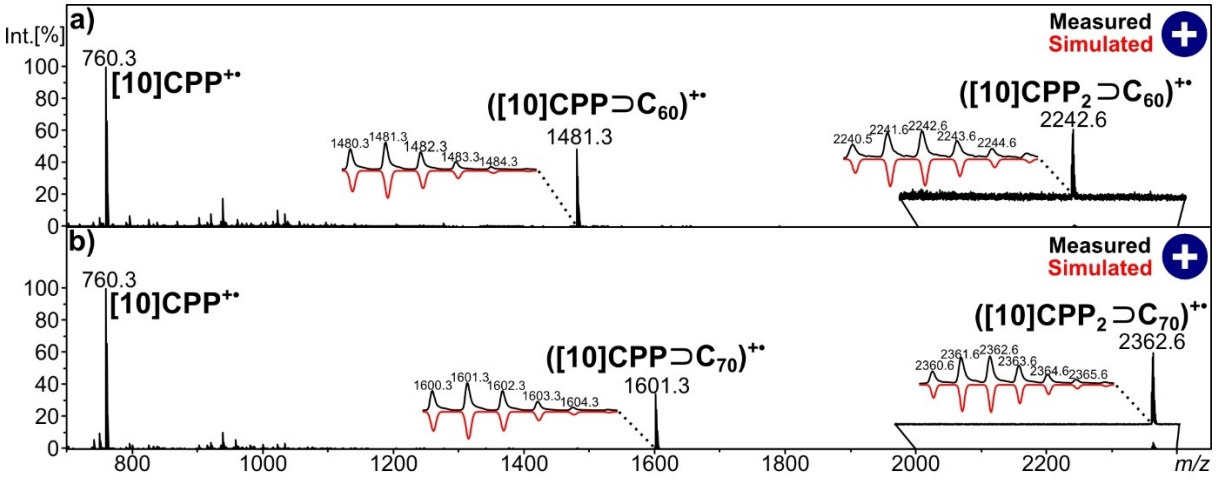

Figure 1. Positive-ion MS^1 spectra of solutions consisting of [10]CPP and a) C_{60} or b) C_{70}.

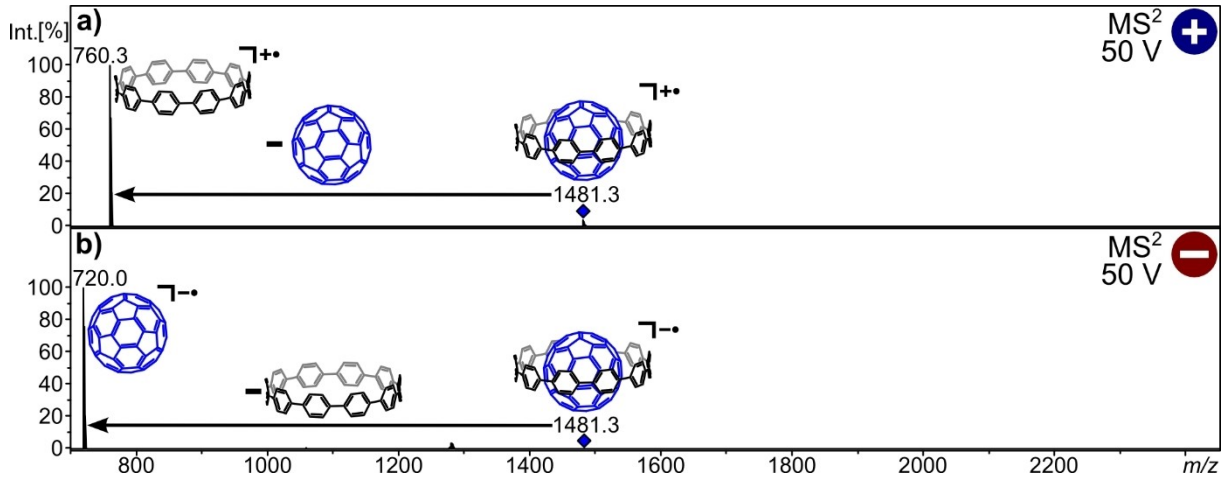

Figure 2. MS^2 spectra of the complex [10]CPP⊃C_{60} in a) positive- and b) negative-ion mode.

cation of the complex. Regarding the negative-ion mode, the radical anion is formed by the introduction of an extra electron into the neutral host-guest complex during the ionization process. Dissociation of the cationic complex leads exclusively to the formation of the [10]CPP radical cation while the C_{60} radical anion is the only fragment ion evolving from dissociation of the anionic host-guest complex. This indicates that, in the case of the cationic complex, the charge resides on the CPP ring upon dissociation. In the anionic complex, on the other hand, the charge is entirely located on the fullerene. The observed charge localization in the radical cation is the result of the lower ionization energy of the nanohoop and has already been reported.[38] The charge distribution in the radical anion originates from the larger electron affinity of the fullerene, facilitating the accommodation of an extra electron. There exists the possibility of charge transfer prior to dissociation. However, we have no indication of it.

The CID mass spectra of the radical cation and anion of the [2:1] complex are displayed in Figures 3a and b, respectively. For both polarities, loss of one neutral [10]CPP ring is the first step and leads to the corresponding charged [1:1] complex ions. These then show the same dissociation behavior as observed for the isolated [1:1] ions (see Figure 2). Regarding the cationic [1:1] complex, we eventually observe the formation of $CPP^{+\bullet}$ via C_{60} release. In the case of the anionic [1:1] complex, $C_{60}^{-\bullet}$ evolves via CPP loss. Such a dissociation in combination with the underlying isotope pattern confirms the [2:1] composition. In turn, it provides the postulated structure, that is, two CPPs noncovalently associated with one fullerene. It also reveals the charge localization within these complexes. Interestingly, we were unable to generate a noncovalent $([10]CPP)_2$ dimer ion in these experiments, which underpins the importance of the fullerene as the central entity to connect the CPPs. We find that the C_{70}-based [1:1] and [2:1] complexes follow the same dissociation behavior as discussed above. The respective spectra are provided in the Supporting Information (see Figures S2 and S3).

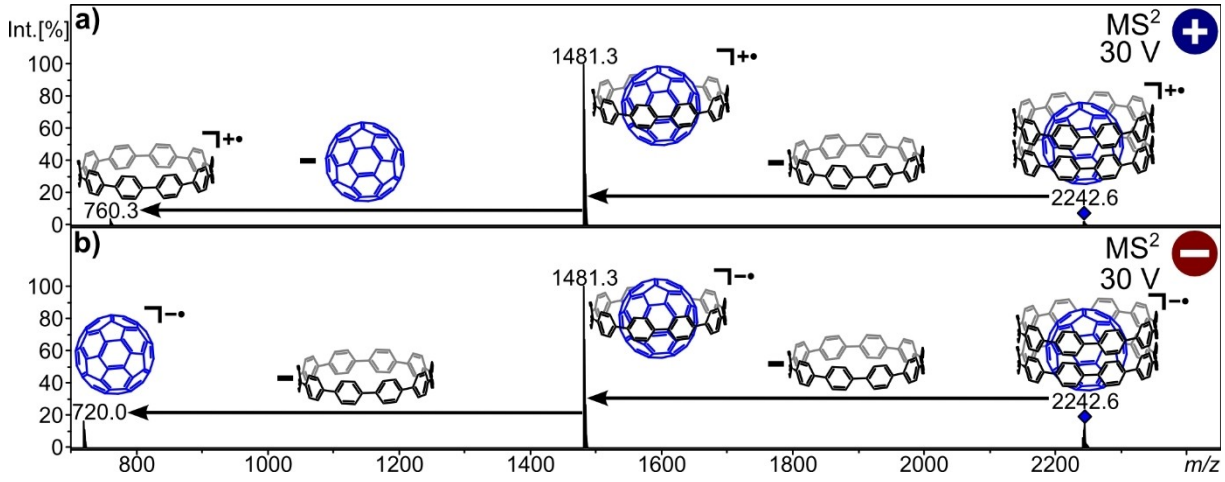

Figure 3. MS^2 spectra of the complex [10]CPP_2⊃C_{60} in a) positive- and b) negative-ion mode.

Next, energy-resolved CID experiments were performed with the [1:1] and [2:1] complex ions. To this end, a selected precursor ion is activated by multiple collisions at well-defined kinetic energies. Conventionally, the total energy that is available for transfer from kinetic into internal energy is determined from the center-of-mass frame and is referred to as center-of-mass collision energy (E_{com}).[58] Using this approach to evaluate the present data led to rather ambiguous results (see Figure S17 and S18). Hence, another way of data processing was deemed important. Semi-empirical molecular dynamics calculations suggest that activation of the complexes leads predominantly to distortions and molecular movements within the much more flexible CPP, while the fullerene remains more or less static (Figures S11–16). Therefore, the dissociation of the complex is primarily caused by structural changes of the CPP ring, while the fullerene remains almost unaffected. This leads to the assumption that the collision energy is initially transferred to the CPP ring rather than the whole complex. To take these considerations into account for the data analysis, the collision energy was derived by dividing the laboratory kinetic energy by the degrees of freedom of the hosting CPP rather than considering the whole complex (E_{lab} DoF^{-1} (CPP)/V). For a more detailed discussion, we refer to section 5 of the Supporting Information.

In the following the bond strengths of the cationic and anionic [1:1] complexes consisting of [10]CPP and $C_{60/70}$ are discussed. The corresponding graphs are shown in Figure 4. We find that dissociation of the radical anion occurs at lower collision energies compared to the respective radical cation, revealing a weaker noncovalent interaction. Furthermore, the complex with C_{70} is in both polarities slightly more stable than the complex with C_{60}. Overall, the following stability trend is obtained for the [1:1] complexes:

$$([10]CPP \supset C_{60})^{-\bullet} < ([10]CPP \supset C_{70})^{-\bullet} \ll ([10]CPP \supset C_{60})^{+\bullet} < ([10]CPP \supset C_{70})^{+\bullet}$$

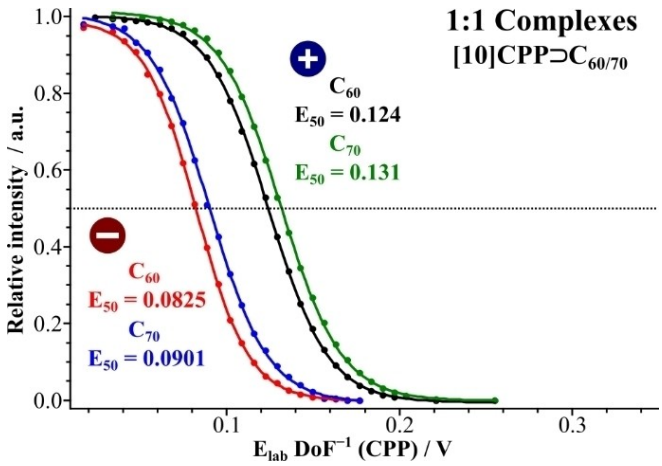

Figure 4. Energy-resolved collision-induced dissociation graphs of positively and negatively charged [10]CPP⊃$C_{60/70}$.

Theoretical investigations of the bond strength between [10]CPP and C_{60}/C_{70} support a stronger binding within the complex of [10]CPP and C_{70}.[38] This is rationalized by the fact that C_{70} features a larger π-system with ovoid geometry than the spherical C_{60}. This enables increased interaction with the nanohoop. Since mass spectrometry relies on ions, DFT calculations were performed with respect to the charged complexes, [10]CPP⊃$C_{60/70}^{-\bullet}$ and [10]CPP⊃$C_{60/70}^{+\bullet}$, thereby accounting for possible influences of the charge (see Supporting Information). For the charged complexes, we observe a similar scenario as for neutral species. In particular, stronger interactions between [10]CPP and fullerene were observed for C_{70} as guest. This observation fits the respective ER-CID measurements. In contrast to the experimental findings, which imply a reduced stability of the anionic complex, theory indicates no difference in bond strength when comparing the cationic and anionic complexes (Table S1 and S2). We attribute the lower stability of the anionic complex to the increased electron density at the fullerene, enhancing repulsive components within the interaction of the π-systems of the host and the guest. In particular, the negatively polarized cavity of the CPP is expected to be repelled by the negative charge of the fullerene.[59–60]

Also, in the case of the [2:1] complexes, the ER-CID measurements (see Figures 5a and b) reveal that both, the charge and the size of the central fullerene, influence the complex stability. Among the studied complexes, the radical cation $([10]CPP)_2 \supset C_{60}^{+\bullet}$ is the least stable while the radical anion of this [2:1] complex shows enhanced stability. The dissociation of C_{70}-based [2:1] complexes occurs at higher collision energies and we find only a small difference between the radical cations and anions. An increased stability of these complexes is caused by the C_{70} core being larger and thereby providing more surface area for interaction with the second CPP ring. The following order of stability applies to the [2:1] complexes:

$$([10]CPP_2 \supset C_{60})^{+\bullet} < ([10]CPP_2 \supset C_{60})^{-\bullet} < ([10]CPP_2 \supset C_{70})^{+\bullet} < ([10]CPP_2 \supset C_{70})^{-\bullet}$$

Considering that all [2:1] complexes decompose in the same manner, that is, they lose one neutral CPP ring as the first step, this stability order reflects the ability of the respective [1:1] complex to accommodate a second CPP.

For the [2:1] complexes, it is possible to deduce important information from the energetic difference between the first and the second fragmentation event. C_{60}-based complexes reveal a relatively large energetic difference between the first and the second fragmentation event, indicating that the second CPP binds only very loosely to the fullerene. For the larger C_{70} core, on the other hand, the energetic difference is not as pronounced since C_{70} can properly bind the neutral CPP in addition to the charged one. For positively charged complexes, the first fragmentation (loss of the neutral CPP) occurs at significantly lower collision energies than the second fragmentation (loss of the positively charged CPP). This clearly shows that the positively charged CPP is preferably bound to the

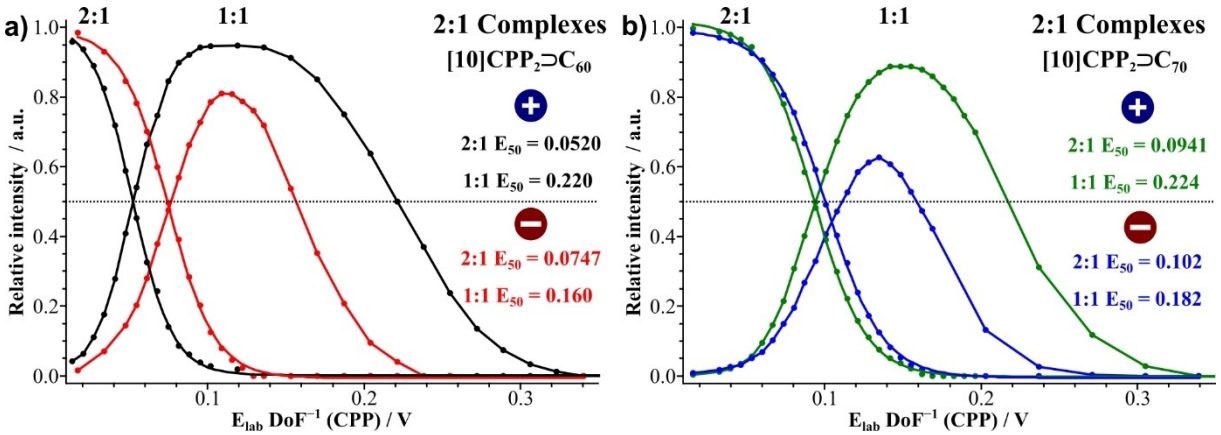

Figure 5. Energy-resolved collision-induced dissociation graphs of positively and negatively charged a) [10]$CPP_2⊃C_{60}$ and b) [10]$CPP_2⊃C_{70}$ complexes.

fullerene. The respective negatively charged complexes show a quite different behavior. Here, the collision energy required for the first and the second fragmentation is almost identical. Such an observation suggests that both CPPs occupy a similar binding site at the negatively charged fullerene.

At first glance, a contradiction results from the observation that [1:1] complexes are more stable as positive ions, while [2:1] complexes show the reversed behavior. A closer look reveals, however, that the instability of the [2:1] cation results from the enhanced stability of the underlying [1:1] complex. This renders the addition of a second CPP ring difficult and facilitates the dissociation of the [2:1] complex to afford the [1:1] complex.

Our calculations also revealed for [2:1] complexes that the magnitude of the fragmentation energy is determined by the size of the fullerene and, hence, the ability of the fullerene to interact with the inner π-system of both nanohoops. Figure 6 illustrates both calculated [2:1] complexes with visualization of the non-covalent interactions (green area).

It becomes evident that C_{70} features a larger interaction surface with both [10]CPPs and forms the more stable complex. Additionally, in both [2:1] complexes dispersion interactions between the hydrogen atoms of the two [10]CPPs are present but play a minor role.

With the formation regarding the respective [1:1] and [2:1] complexes in the gas-phase and by DFT studies at hand, the question arose whether this is transferrable to solution. Thus, we turned to complex formation in 1,2-dichlorobenzene (*o*-DCB) using ITC. This technique has been proven to be a very powerful tool to study the complexation between fullerene derivatives and strained carbon nanohoops, thereby providing the binding affinities, stoichiometries and thermodynamic parameters of the complex formation.[45] The titrations were performed in two different ways. First, the [10]CPP concentration was kept constant and increasing amounts of $C_{60/70}$ were added in order to favour the formation of the [1:1] complex, as shown in the thermograms of Figures 7a and c. Second, titrations with a constant concentration of $C_{60/70}$ and an excess of [10]CPP were performed to promote the formation of the [2:1] complexes (Figures 7b and d).

The global analysis of the triplicate titration with the independent sites binding model revealed a stoichiometry close to 1 ($n = 0.986$) and a binding constant $K_a = 2.49 \cdot 10^5\ M^{-1}$ for [10]CPP⊃C_{60} and $n = 0.735$ and $K_a = 6.20 \cdot 10^4\ M^{-1}$ for

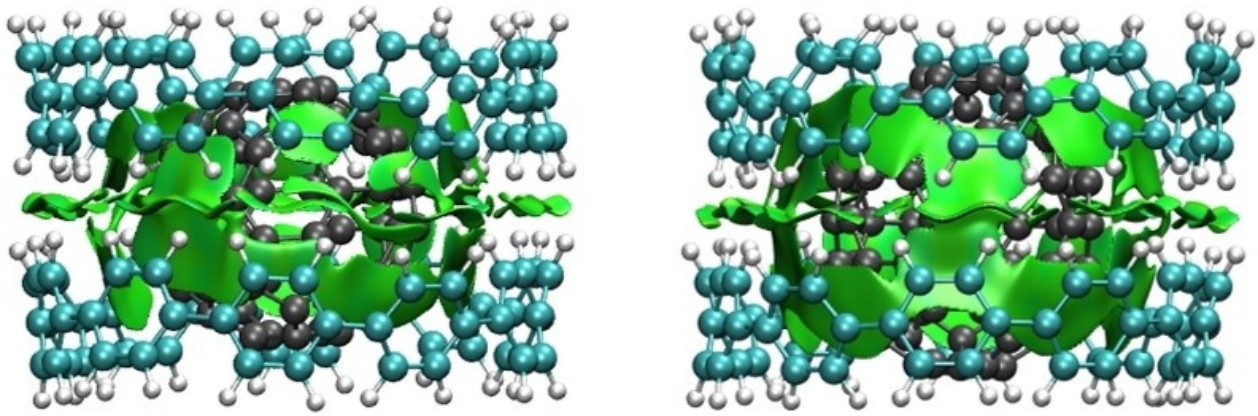

Figure 6. Optimized geometries of [10]$CPP_2⊃C_{60}$ (left) and [10]$CPP_2⊃C_{70}$ (right) complexes with visualization of the non-covalent interactions.

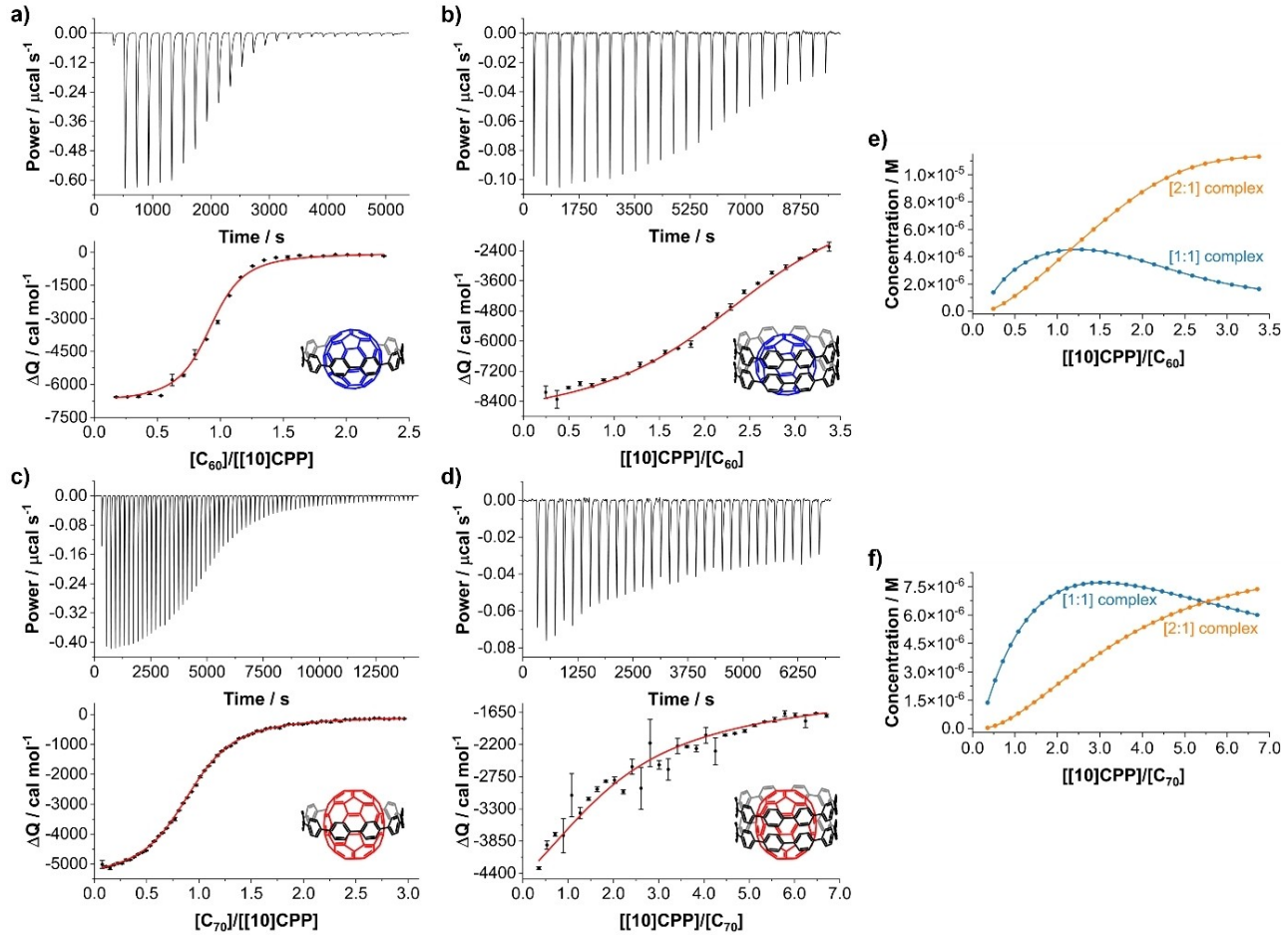

Figure 7. Thermograms and corresponding binding fittings using the independent model from the ITC titrations in *o*-DCB. a) and c) [10]CPP⊃$C_{60/70}$, b) and d) [10]CPP_2⊃$C_{60/70}$ (solubility limitations hampered ideal host-guest titrations and optimal sigmoidal curves could not be obtained). e) and f) species evolution upon titration using the stoichiometric 2:1 binding model.

[10]CPP⊃C_{70} as [1:1] complexes (see Table 1 and Figures 7a and 7b, respectively). Notably, the affinity trend observed in *o*-DCB is reversed to that found in our gas-phase experiments. The higher solubility of C_{70} in *o*-DCB (C_{60} 24.6 g L^{-1} versus 36.2 g L^{-1} for C_{70} in *o*-DCB)[61,62] plays a fundamental role in the binding process. Previous experiments in toluene also confirm a higher [10]CPP affinity for C_{60} (compared to C_{70}).[39,41] Nevertheless, a reversed "affinity trend" in both of these experiments is no contradiction at all. Gas-phase collision experiments refer to the dissociation of the pre-formed complex. Solution-phase titration experiments relate to its equilibrium formation in solution.

Analysis of those titrations that featured an excess of [10]CPP unambiguously corroborated the formation of the [2:1] complexes. The stoichiometry is very close to 2 for both fullerenes, that is, n = 1.910 for C_{60} and n = 2.073 for C_{70} (Table 1 and Figures 7b and d). Further analysis by means of the stoichiometric approach to consider a [2:1] binding model (Table 2 and Figures S4-7 for standard deviations and fitting details) offered the differences in binding affinities for the first and second CPP ring and allows to follow the species distribution upon titration (Figures 7e and f). As shown in Figure 7e, the formation of [10]CPP_2⊃C_{60} predominates the process after addition of more than 2 equivalents of [10]CPP. The binding constants for the first and second binding event $K_{a,1}$ and $K_{a,2}$ are in the same order of magnitude (Table 2) with $K_{a,2}$ being slightly larger than $K_{a,1}$. For C_{70}, a significant excess of

Table 1. Thermodynamic parameters obtained from the ITC fitted with the independent sites model.

System	K_a [1/M]	ΔH [cal/mol]	ΔG [cal/mol]	ΔS [cal/mol*K]	n
C_{60} into [10]CPP	$(2.49 \pm 0.23) \cdot 10^5$	$-(6.16 \pm 0.49) \cdot 10^3$	$-7.36 \cdot 10^3$	4.01	0.986 ± 0.09
[10]CPP into C_{60}		$-(9.17 \pm 0.16) \cdot 10^3$		−6.08	1.910 ± 0.23
C_{70} into [10]CPP	$(6.20 \pm 0.87) \cdot 10^4$	$-(6.87 \pm 1.96) \cdot 10^3$	$-6.54 \cdot 10^3$	−1.11	0.735 ± 0.11
[10]CPP into C_{70}		$-(3.64 \pm 0.49) \cdot 10^3$		9.72	2.073 ± 0.13

Table 2. Thermodynamic parameters obtained from the ITC data fitted with the [2:1] stoichiometric model.

System	K_a [1/M][a]	ΔH [cal/mol]	ΔG [cal/mol]	ΔS [cal/mol*K]
[10]CPP into C_{60}	$K_{a,1} = 2.46 \cdot 10^5$	$-(6.33 \pm 0.07) \cdot 10^3$	$-7.35 \cdot 10^3$	3.44
	$K_{a,2} = (3.79 \pm 0.07) \cdot 10^5$	$-(8.54 \pm 0.00) \cdot 10^3$	$-7.61 \cdot 10^3$	−3.13
[10]CPP into C_{70}	$K_{a,1} = 4.56 \cdot 10^4$	$-(5.05 \pm 0.00) \cdot 10^3$	$-6.35 \cdot 10^3$	4.37
	$K_{a,2} = (1.89 \pm 0.07) \cdot 10^4$	$-(3.30 \pm 1.89) \cdot 10^2$	$-5.83 \cdot 10^3$	18.5

[a] For the global fitting $K_{a,1}$ was set to the K_a value received from a previous fitting of the triple titration of C_{60}/C_{70} into [10]CPP evaluated with the 1:1 binding model, which is why there is no error given for this first binding constant.

[10]CPP (ca. 6 equivalents) is needed so that [10]$CPP_2 \supset C_{70}$ outweighs [10]$CPP \supset C_{70}$ in solution (Figure 7f). This stems from the lower affinity of binding the second [10]CPP (Table 2). Interestingly, the second [10]CPP binding to C_{70} shows an inversion in the entropic contribution with respect to the C_{60} fullerene, which becomes positive. This fact reflects again the above mentioned solubility differences, which might also be related to solvophobic effects. Furthermore, the ovoid shape of C_{70} implies a larger influence of the relative orientation in the complex formation and might also play a role in the entropic term. Nevertheless, in absolute values the entropic contribution (cal/mol) is almost negligible in comparison to the enthalpic term (kcal/mol). Overall, and in view of the thermodynamic parameters obtained, the binding for both [1:1] and [2:1] complexes is an exothermic and enthalpy-driven process.

Conclusion

Using APPI and ESI mass spectrometry in positive- and negative-ion mode, we successfully investigated literature-known [1:1] complexes between [10]CPP and $C_{60/70}$ as well as the novel [2:1] complexes consisting of two [10]CPPs and one fullerene. In addition, our experimental findings are supported by theoretical calculations.

Energy-dependent collision experiments were performed to examine the charge distribution and the dissociation behavior of the [1:1] complexes. In the case of the positively charged complexes, the charge is solely located at the [10]CPP while for negatively charged complexes the charge resides at the fullerene. This is due to the lower ionization energy of [10]CPP and the higher electron affinity of the fullerenes. Regarding the stability of the [1:1] complexes, we find that C_{60}-based complexes are less stable than the respective C_{70} analogues and that the radical cations are more stable than the negatively charged complexes.

The fragmentation of the [2:1] complexes proceeds stepwise. First, one neutral [10]CPP is released, thereby forming the corresponding [1:1] complex. Subsequently, the dissociation of the [1:1] complexes occurs. It can also be seen that C_{70} as the central entity yields more stable [2:1] complexes as its larger dimension allows for stronger binding of the second [10]CPP. Contrary to the [1:1] complexes, the [2:1] complexes exhibit a greatly reduced stability of the radical cation, which results from the high stability of the corresponding positively charged [1:1] complex.

Additionally, the presence of the [1:1] and [2:1] complexes was unambiguously confirmed in solution using ITC revealing the corresponding stoichiometries and thermodynamic parameters. The gas-phase experiments and DFT calculations reveal a somewhat more pronounced stability of the C_{70} complex, while equilibrium formation in solution prefers the complexation with C_{60} (with K_a ranging from 10^4 to 10^5 M^{-1}). However, the stoichiometry of $n = 2$ as well as the species evolution upon titration corroborated the formation of [10]$CPP_2 \supset C_{60}$ and [10]$CPP_2 \supset C_{70}$ complexes during an exothermic and enthalpy-driven process.

This study provides new insights into the gas-phase and solution chemistry of [10]CPP with $C_{60/70}$, thereby contributing to a detailed understanding of the fascinating host-guest chemistry of fullerenes and nanohoops.

Acknowledgements

The authors acknowledge financial support by the Deutsche Forschungsgemeinschaft (DFG) SFB953 "Synthetic Carbon Allotropes", Projektnummer 182849149. The authors thank the computational resources and support provided by the Erlangen Regional Computing Center (RRZE). M.F. acknowledges financial support by the Hanns-Seidel-Stiftung. Open Access funding enabled and organized by Projekt DEAL.

Conflict of Interest

The authors declare no conflict of interest.

Data Availability Statement

The data that support the findings of this study are available from the corresponding author upon reasonable request.

Keywords: cycloparaphenylenes · fullerenes · host-guest systems · polycyclic aromatic hydrocarbons · supramolecular chemistry

[1] P. Bäuerle, M. Ammann, M. Wilde, G. Götz, E. Mena-Osteritz, A. Rang, C. A. Schalley, *Angew. Chem. Int. Ed.* **2007**, *46*, 363–368; *Angew. Chem.* **2007**, *119*, 367–372.

[2] Y.-Y. Fan, D. Chen, Z.-A. Huang, J. Zhu, C.-H. Tung, L.-Z. Wu, H. Cong, *Nat. Commun.* **2018**, *9*, 3037.
[3] Y. Segawa, M. Kuwayama, Y. Hijikata, M. Fushimi, T. Nishihara, J. Pirillo, J. Shirasaki, N. Kubota, K. Itami, *Science* **2019**, *365*, 272–276.
[4] Y. Segawa, M. Kuwayama, K. Itami, *Org. Lett.* **2020**, *22*, 1067–1070.
[5] W. Zhang, A. Abdulkarim, F. E. Golling, H. J. Räder, K. Müllen, *Angew. Chem. Int. Ed.* **2017**, *56*, 2645–2648; *Angew. Chem.* **2017**, *129*, 2689–2692.
[6] E. R. Darzi, T. J. Sisto, R. Jasti, *J. Org. Chem.* **2012**, *77*, 6624–6628.
[7] T. Iwamoto, Y. Watanabe, Y. Sakamoto, T. Suzuki, S. Yamago, *J. Am. Chem. Soc.* **2011**, *133*, 8354–8361.
[8] Y. Segawa, A. Fukazawa, S. Matsuura, H. Omachi, S. Yamaguchi, S. Irle, K. Itami, *Org. Biomol. Chem.* **2012**, *10*, 5979–5984.
[9] P. Li, T. J. Sisto, E. R. Darzi, R. Jasti, *Org. Lett.* **2014**, *16*, 182–185.
[10] M. Fujitsuka, T. Iwamoto, E. Kayahara, S. Yamago, T. Majima, *ChemPhysChem* **2013**, *14*, 1570–1572.
[11] D. A. Hines, E. R. Darzi, R. Jasti, P. V. Kamat, *J. Phys. Chem. A* **2014**, *118*, 1595–1600.
[12] E. J. Leonhardt, R. Jasti, *Nat. Chem. Rev.* **2019**, *3*, 672–686.
[13] Y. Xu, M. von Delius, *Angew. Chem. Int. Ed.* **2020**, *59*, 559–573; *Angew. Chem.* **2020**, *132*, 567–582.
[14] R. Jasti, J. Bhattacharjee, J. B. Neaton, C. R. Bertozzi, *J. Am. Chem. Soc.* **2008**, *130*, 17646–17647.
[15] H. Takaba, H. Omachi, Y. Yamamoto, J. Bouffard, K. Itami, *Angew. Chem. Int. Ed.* **2009**, *48*, 6112–6116; *Angew. Chem.* **2009**, *121*, 6228–6232.
[16] D. Wassy, M. Pfeifer, B. Esser, *J. Org. Chem.* **2020**, *85*, 34–43.
[17] M. Hermann, D. Wassy, J. Kohn, P. Seitz, M. U. Betschart, S. Grimme, B. Esser, *Angew. Chem. Int. Ed.* **2021**, *60*, 10680–10689; *Angew. Chem.* **2021**, *133*, 10775–10784.
[18] J. S. Wössner, D. Wassy, A. Weber, M. Bovenkerk, M. Hermann, M. Schmidt, B. Esser, *J. Am. Chem. Soc.* **2021**, *143*, 12244–12252.
[19] J. Xia, M. R. Golder, M. E. Foster, B. M. Wong, R. Jasti, *J. Am. Chem. Soc.* **2012**, *134*, 19709–19715.
[20] Y. Ishii, S. Matsuura, Y. Segawa, K. Itami, *Org. Lett.* **2014**, *16*, 2174–2176.
[21] E. Kayahara, R. Qu, S. Yamago, *Angew. Chem. Int. Ed.* **2017**, *56*, 10428–10432; *Angew. Chem.* **2017**, *129*, 10564–10568.
[22] E. J. Leonhardt, J. M. Van Raden, D. Miller, L. N. Zakharov, B. Alemán, R. Jasti, *Nano Lett.* **2018**, *18*, 7991–7997.
[23] S. Hashimoto, E. Kayahara, Y. Mizuhata, N. Tokitoh, K. Takeuchi, F. Ozawa, S. Yamago, *Org. Lett.* **2018**, *20*, 5973–5976.
[24] Y. Xu, B. Wang, R. Kaur, M. B. Minameyer, M. Bothe, T. Drewello, D. M. Guldi, M. von Delius, *Angew. Chem. Int. Ed.* **2018**, *57*, 11549–11553; *Angew. Chem.* **2018**, *130*, 11723–11727.
[25] J. M. Van Raden, E. J. Leonhardt, L. N. Zakharov, A. Pérez-Guardiola, A. J. Pérez-Jiménez, C. R. Marshall, C. K. Brozek, J. C. Sancho-García, R. Jasti, *J. Org. Chem.* **2020**, *85*, 129–141.
[26] H. Shudo, M. Kuwayama, M. Shimasaki, T. Nishihara, Y. Takeda, N. Mitoma, T. Kuwabara, A. Yagi, Y. Segawa, K. Itami, *Nat. Commun.* **2022**, *13*, 3713.
[27] K. Matsui, Y. Segawa, K. Itami, *Org. Lett.* **2012**, *14*, 1888–1891.
[28] E. R. Darzi, E. S. Hirst, C. D. Weber, L. N. Zakharov, M. C. Lonergan, R. Jasti, *ACS Cent. Sci.* **2015**, *1*, 335–342.
[29] J. M. Van Raden, E. R. Darzi, L. N. Zakharov, R. Jasti, *Org. Biomol. Chem.* **2016**, *14*, 5721–5727.
[30] J. M. Van Raden, S. Louie, L. N. Zakharov, R. Jasti, *J. Am. Chem. Soc.* **2017**, *139*, 2936–2939.
[31] M. Chen, K. S. Unikela, R. Ramalakshmi, B. Li, C. Darrigan, A. Chrostowska, S.-Y. Liu, *Angew. Chem. Int. Ed.* **2021**, *60*, 1556–1560; *Angew. Chem.* **2021**, *133*, 1580–1584.
[32] F. Schwer, S. Zank, M. Freiberger, R. Kaur, S. Frühwald, C. C. Robertson, A. Görling, T. Drewello, D. M. Guldi, M. Von Delius, *Organic Materials* **2022**, *4(02)*, 7–17.
[33] M. Hermann, D. Wassy, B. Esser, *Angew. Chem. Int. Ed.* **2021**, *60*, 15743–15766; *Angew. Chem.* **2021**, *133*, 10775–10784.
[34] J. Wang, X. Zhang, H. Jia, S. Wang, P. Du, *Acc. Chem. Res.* **2021**, *54*, 4178–4190.
[35] S. Hashimoto, T. Iwamoto, D. Kurachi, E. Kayahara, S. Yamago, *ChemPlusChem* **2017**, *82*, 1015–1020.
[36] C. Zhao, H. Meng, M. Nie, X. Wang, Z. Cai, T. Chen, D. Wang, C. Wang, T. Wang, *J. Phys. Chem. C* **2019**, *123*, 12514–12520.
[37] C. Zhao, F. Liu, L. Feng, M. Nie, Y. Lu, J. Zhang, C. Wang, T. Wang, *Nanoscale* **2021**, *13*, 4880–4886.
[38] M. B. Minameyer, Y. Xu, S. Frühwald, A. Görling, M. von Delius, T. Drewello, *Chem. Eur. J.* **2020**, *26*, 8729–8741.
[39] T. Iwamoto, Y. Watanabe, T. Sadahiro, T. Haino, S. Yamago, *Angew. Chem. Int. Ed.* **2011**, *50*, 8342–8344; *Angew. Chem.* **2011**, *123*, 8492–8494.
[40] J. Xia, J. W. Bacon, R. Jasti, *Chem. Sci.* **2012**, *3*, 3018–3021.
[41] T. Iwamoto, Y. Watanabe, H. Takaya, T. Haino, N. Yasuda, S. Yamago, *Chem. Eur. J.* **2013**, *19*, 14061–14068.
[42] E. Ubasart, O. Borodin, C. Fuertes-Espinosa, Y. Xu, C. García-Simón, L. Gómez, J. Juanhuix, F. Gándara, I. Imaz, D. Maspoch, M. von Delius, X. Ribas, *Nat. Chem.* **2021**, *13*, 420–427.
[43] A. Stergiou, J. Rio, J. H. Griwatz, D. Arčon, H. A. Wegner, C. P. Ewels, N. Tagmatarchis, *Angew. Chem. Int. Ed.* **2019**, *58*, 17745–17750; *Angew. Chem.* **2019**, *131*, 17909–17914.
[44] J. Rio, S. Beeck, G. Rotas, S. Ahles, D. Jacquemin, N. Tagmatarchis, C. Ewels, H. A. Wegner, *Angew. Chem. Int. Ed.* **2018**, *57*, 6930–6934; *Angew. Chem.* **2018**, *130*, 7046–7050.
[45] I. Solymosi, J. Sabin, H. Maid, L. Friedrich, E. Nuin, M. E. Perez-Ojeda, A. Hirsch, *Organic Materials* **2022**, *4(03)*, 73–85.
[46] Y. Xu, R. Kaur, B. Wang, M. B. Minameyer, S. Gsänger, B. Meyer, T. Drewello, D. M. Guldi, M. von Delius, *J. Am. Chem. Soc.* **2018**, *140*, 13413–13420.
[47] Y. Tanuma, A. Stergiou, A. Bužan Bobnar, M. Gaboardi, J. Rio, J. Volkmann, H. A. Wegner, N. Tagmatarchis, C. P. Ewels, D. Arčon, *Nanoscale* **2021**, *13*, 19946–19955.
[48] T. Iwamoto, Z. Slanina, N. Mizorogi, J. Guo, T. Akasaka, S. Nagase, H. Takaya, N. Yasuda, T. Kato, S. Yamago, *Chem. Eur. J.* **2014**, *20*, 14403–14409.
[49] H. Ueno, T. Nishihara, Y. Segawa, K. Itami, *Angew. Chem. Int. Ed.* **2015**, *54*, 3707–3711; *Angew. Chem.* **2015**, *127*, 3778–3782.
[50] Y. Nakanishi, H. Omachi, S. Matsuura, Y. Miyata, R. Kitaura, Y. Segawa, K. Itami, H. Shinohara, *Angew. Chem. Int. Ed.* **2014**, *53*, 3102–3106; *Angew. Chem.* **2014**, *126*, 3166–3170.
[51] J. Zhang, C. Zhao, H. Meng, M. Nie, Q. Li, J. Xiang, Z. Zhang, C. Wang, T. Wang, *Carbon* **2020**, *161*, 694–701.
[52] J. Liang, Y. Lu, J. Zhang, L. Qiu, W. Li, Z. Zhang, C. Wang, T. Wang, *Dalton Trans.* **2022**, *51*, 10227–10233.
[53] T. Matsuno, M. Fujita, K. Fukunaga, S. Sato, H. Isobe, *Nat. Commun.* **2018**, *9*, 3779.
[54] S. Adachi, M. Shibasaki, N. Kumagai, *Nat. Commun.* **2019**, *10*, 3820.
[55] H. Kwon, C. J. Bruns, *Nano Res.* **2022**, *15*, 5545–5555.
[56] D. Lu, G. Zhuang, H. Jia, J. Wang, Q. Huang, S. Cui, P. Du, *Org. Chem. Front.* **2018**, *5*, 1446–1451.
[57] Y. Xu, S. Gsänger, M. B. Minameyer, I. Imaz, D. Maspoch, O. Shyshov, F. Schwer, X. Ribas, T. Drewello, B. Meyer, M. von Delius, *J. Am. Chem. Soc.* **2019**, *141*, 18500–18507.
[58] A. K. Shukla, J. H. Futrell, *J. Mass Spectrom.* **2000**, *35*, 1069–1090.
[59] L. T. Scott, *Angew. Chem. Int. Ed.* **2003**, *42*, 4133–4135; *Angew. Chem.* **2003**, *42*, 4133–4135.
[60] I. González-Veloso, E. M. Cabaleiro-Lago, J. Rodríguez-Otero, *Phys. Chem. Chem. Phys.* **2018**, *20*, 11347–11358.
[61] J. M. T. Walter A. Scrivens, *J. Chem. Soc. Chem. Commun.* **1993**, 1207–1209.
[62] N. Sivaraman, R. Dhamodaran, I. Kaliappan, T. G. Srinivasan, P. R. P. Vasudeva Rao, C. K. C. Mathews, *Fullerene Sci. Technol.* **1994**, *2*, 233–246.

Manuscript received: November 30, 2022
Accepted manuscript online: December 12, 2022
Version of record online: February 10, 2023